



Individual *Microcystis* colonies harbour distinct bacterial communities that differ by *Microcystis* oligotype and with time

Derek J. Smith ¹, James Y. Tan,²
McKenzie A. Powers,¹ Xiaoxia N. Lin,²
Timothy W. Davis³ and Gregory J. Dick ^{1*}

¹Department of Earth & Environmental Science, The University of Michigan, 1100 N. University Building, 1100 N. University Avenue, Ann Arbor, MI, 48109.

²Department of Chemical Engineering, The University of Michigan, NCRC, 2800 Plymouth Rd., Ann Arbor, MI, 48109.

³Department of Biological Sciences, Bowling Green State University, Life Sciences Building, Corner of N. College Dr and E. Merry Avenue, Bowling Green, OH, 43403.

Summary

Interactions between bacteria and phytoplankton in the phycosphere have impacts at the scale of whole ecosystems, including the development of harmful algal blooms. The cyanobacterium *Microcystis* causes toxic blooms that threaten freshwater ecosystems and human health globally. *Microcystis* grows in colonies that harbour dense assemblages of other bacteria, yet the taxonomic composition of these phycosphere communities and the nature of their interactions with *Microcystis* are not well characterized. To identify the taxa and compositional variance within *Microcystis* phycosphere communities, we performed 16S rRNA V4 region amplicon sequencing on individual *Microcystis* colonies collected biweekly via high-throughput droplet encapsulation during a western Lake Erie cyanobacterial bloom. The *Microcystis* phycosphere communities were distinct from microbial communities in whole water and bulk phytoplankton seston in western Lake Erie but lacked ‘core’ taxa found across all colonies. However, dissimilarity in phycosphere community composition correlated with sampling date and the *Microcystis*

16S rRNA oligotype. Several taxa in the phycosphere were specific to and conserved with *Microcystis* of a single oligotype or sampling date. Together, this suggests that physiological differences between *Microcystis* strains, temporal changes in strain phenotypes, and the composition of seeding communities may impact community composition of the *Microcystis* phycosphere.

Introduction

Microbial interactions play a central role in many biogeochemical processes and have ecosystem wide impacts. A familiar example is the interaction between phytoplankton and heterotrophic bacteria, which can often be mutualistic. Specifically, phytoplankton provide organic carbon and sulfur that support heterotrophic bacterial growth while their heterotrophic partners improve phytoplankton growth by producing essential vitamins and growth promoters (Croft *et al.*, 2005; Amin *et al.*, 2015; Durham *et al.*, 2015; Durham *et al.*, 2017), increasing the bioavailability of trace metals (Amin *et al.*, 2009; Basu *et al.*, 2019), regenerating nutrients from organic material (Van Mooy *et al.*, 2012; Amin *et al.*, 2015; Arandia-Gorostidi *et al.*, 2017; Christie-Oleza *et al.*, 2017), and detoxifying reactive oxygen species (Morris *et al.*, 2011; Ma *et al.*, 2018).

Many phytoplankton-bacteria interactions occur in close proximity or with physical attachment of the interacting cells (Paerl and Gallucci, 1985; Segev *et al.*, 2016; Arandia-Gorostidi *et al.*, 2017; Frischkorn *et al.*, 2017) within a zone of interaction called the phycosphere (Bell and Mitchell, 1972; Cole, 1982; Seymour *et al.*, 2017). The phycosphere is rich in dissolved organic carbon (DOC) exuded by phytoplankton or released upon cell lysis, which attracts chemotactic bacteria (Bell and Mitchell, 1972; Paerl and Gallucci, 1985; Barbara and Mitchell, 2003; Sonnenschein *et al.*, 2012; Smriga *et al.*, 2016). Interactions within the phycosphere can take place between conserved heterotrophic community members and phytoplankton taxa (Jasti *et al.*, 2005; Sison-Mangus *et al.*, 2014; Durham *et al.*, 2015;

Received 8 August, 2020; revised 11 March, 2021; accepted 6 April, 2021. *For correspondence. E-mail: gdick@umich.edu; Tel. 734 763 3228; Fax. 734-763-4690.

Frischkorn *et al.*, 2017; Lee *et al.*, 2017). The recruitment of specific heterotrophic taxa may be driven by the production of signalling-molecules (Durham *et al.*, 2015; Segev *et al.*, 2016; Durham *et al.*, 2017) or through the unique exometabolomes of each phytoplankton taxon (Bell and Mitchell, 1972; Seymour *et al.*, 2010; Landa *et al.*, 2017), which may elicit chemotactic responses in specific taxa (Bell and Mitchell, 1972; Bassler *et al.*, 1991; Miller *et al.*, 2004). Interactions within the phycosphere have impacts at the scale of whole ecosystems (Azam and Malfatti, 2007; Seymour *et al.*, 2017), such as driving carbon cycling (Smriga *et al.*, 2016) or algal bloom development and termination (Seyedsayamdost *et al.*, 2011) in marine systems.

While a growing body of literature has characterized phycosphere interactions between marine taxa (Ferrier *et al.*, 2002; Jasti *et al.*, 2005; Sison-Mangus *et al.*, 2014; Amin *et al.*, 2015; Segev *et al.*, 2016; Frischkorn *et al.*, 2017), comparatively little work has been conducted in freshwater systems despite their importance for recreation, fisheries, biodiversity, agriculture, and drinking water. Globally, freshwaters are increasingly threatened by cyanobacterial harmful algal blooms (CHABs) due to anthropogenic nutrient pollution and global climate change (Huisman *et al.*, 2018). *Microcystis* is a globally dominant cyanobacterium in many freshwater CHABs, and some strains produce microcystins, a class of potent hepatotoxins that can cause liver damage and death in mammals when ingested (Harke *et al.*, 2016). *Microcystis* spp. grow in large, buoyant colonies (50–1000 µm diameter) (Zhu *et al.*, 2014) that can be either clonal or nonclonal (Otten *et al.*, 2017; Jackrel *et al.*, 2019) and harbour other bacteria (Hindák, 1996; Worm and Søndergaard, 1998). Studies on bulk phytoplankton aggregates dominated by *Microcystis* suggest that the bacterial communities associated with *Microcystis* colonies are distinct from those associated with other cyanobacteria and free-living communities in the surrounding water column (Parveen *et al.*, 2013; Louati *et al.*, 2015; Zhu *et al.*, 2019; Jankowiak and Gobler, 2020). Interactions between other phytoplankton and bacteria influence the growth and toxin production of marine harmful algal blooms (Ferrier *et al.*, 2002; Adachi *et al.*, 2003; Sison-Mangus *et al.*, 2014), with some strain and species specific effects (Sison-Mangus *et al.*, 2014), and bacteria can influence the invasion capability of some *Microcystis* strains into established green algae cultures (Schmidt *et al.*, 2020). Together, these observations suggest that bacteria associated with *Microcystis* could affect the relative fitness and proportion of *Microcystis* strains, which is an important determinant of toxin concentrations in *Microcystis* blooms (Kardinaal *et al.*, 2007; Davis *et al.*, 2009; Davis *et al.*, 2010; Otten *et al.*, 2012). While

previous studies have characterized heterotrophic bacteria populations in enrichment culture with *Microcystis* (Jackrel *et al.*, 2019; Kim *et al.*, 2019) or in total communities during blooms (Parveen *et al.*, 2013; Louati *et al.*, 2015; Berry *et al.*, 2017a; Shi *et al.*, 2018; Chun *et al.*, 2019; Kim *et al.*, 2019; Zhu *et al.*, 2019; Chun *et al.*, 2020; Cook *et al.*, 2020; Jankowiak and Gobler, 2020), the microbes that comprise natural *Microcystis* colonies and the variation in community composition across individual colonies are comparatively understudied. To our knowledge, only two studies have identified the bacterial communities associated with single *Microcystis* colonies (Shia *et al.*, 2010; Tu *et al.*, 2019). Both were limited to single time points and low numbers of colonies, and one did not deeply characterize colony-associated communities with high-throughput sequencing (Shia *et al.*, 2010). Therefore, the extent to which *Microcystis* phycosphere communities on individual colonies vary across strains and species of *Microcystis* and with time and space is unknown.

In order to characterize the bacterial communities associated with the *Microcystis* phycosphere, we isolated single *Microcystis* colonies from a western Lake Erie CHAB in 2019 via droplet encapsulation, which provides higher throughput and precision than traditional methods of colony isolation. We then performed amplicon sequencing of the V4 region of the bacterial 16S rRNA genes. With the resulting dataset, we focus on answering the following questions: (1) Do *Microcystis* colonies harbour taxa that are universal, comprising a 'core' phycosphere community? (2) How do *Microcystis* phycosphere communities vary between individual colonies? (3) How do *Microcystis* phycosphere communities change throughout bloom development? We found that *Microcystis* colonies harbour phycosphere communities that are distinct from whole water bacterial communities and bulk phytoplankton seston communities (100 µm retentate, including *Microcystis* colonies), and differ by sampling date and *Microcystis* oligotype. We hypothesize that these distinct phycosphere communities are shaped by strain-specific interactions as well as changes in either seeding communities or the physicochemical environment over time.

Results and discussion

Microcystis colony oligotype assignment

MED analysis showed that the *Microcystis* sequences in each colony were primarily composed of either a single oligotype or two oligotypes at approximately equal proportions (Fig. S3A). We interpret that the colonies with primarily two oligotypes represent clonal colonies

comprised of *Microcystis* strains with two distinct 16S rRNA gene copies, while the colonies with primarily one oligotype represent clonal *Microcystis* colonies comprised of strains with two identical V4 regions of the 16S rRNA gene. Although some atypical colonies can form from aggregation of multiple strains (Otten *et al.*, 2017; Jackrel *et al.*, 2019), *Microcystis* colonies from eutrophic environments are primarily clonal (Jackrel *et al.*, 2019). Furthermore, if colonies were composed of multiple *Microcystis* strains, the proportions of the MED nodes should be more variable across the sequenced colonies. Inspection of all publicly available and closed *Microcystis* genomes ($n = 9$) confirmed that all have two 16S rRNA gene copies. Pairwise alignment of the two gene copies from each genome showed that the shared nucleotide composition of the gene copies varies between *Microcystis* strains, and the nucleotide sequence variation occurred at different nucleotide positions in each strain (Table S1). From these MED results, we classified the colonies into oligotype groups based on their pair of sequence variants (see Experimental procedures). While oligotypes do not perfectly represent all genotypic differences between closely related bacterial strains (Berry *et al.*, 2017b), oligotyping has been shown to identify closely related sequence variants that covary along environmental and biological gradients while ignoring artifactual sequence variation (Eren *et al.*, 2013; Eren *et al.*, 2014; Berry *et al.*, 2017b). Here, we use *Microcystis* oligotypes as an approximation of closely related *Microcystis* strains/species.

There were temporal trends in the relative proportions of the *Microcystis* oligotypes among the sampled colonies (Fig. S3B). Oligotype 3 colonies accounted for a greater proportion of the total colonies sampled in August and were absent in September. While oligotype 1 colonies were present on every date, they were a larger fraction of the total colonies sampled in September. Oligotype 2 colonies were only sampled in September. The temporal trends in oligotype representation are not correlated with the abundance of the major *Microcystis* MED nodes that

comprise colony oligotypes 1 and 3 in the whole water microbial communities; these *Microcystis* MED nodes showed similar temporal trends in their abundance and were present at similar concentrations in whole water (Fig. S4).

Microcystis phycosphere community diversity

Microscopy showed that *Microcystis* colonies from western Lake Erie are densely packed with small, non-*Microcystis* bacterial cells (Fig. 1). Amplicon sequencing of individual colonies revealed the presence of many different non-*Microcystis* taxa, some of which occurred frequently at high relative abundance across different colonies (Fig. 2). In total, we identified 197 different non-*Microcystis* operational taxonomic units (OTUs) in the phycosphere. Of all the non-*Microcystis* OTUs identified in the phycosphere, the most frequently occurring and abundant were from the Bacteroidetes, Alphaproteobacteria, Betaproteobacteria and Cyanobacteria as previously observed in bulk colony samples (Parveen *et al.*, 2013; Louati *et al.*, 2015; Shi *et al.*, 2018; Zhu *et al.*, 2019). There were also abundant but less frequent OTUs from the Acidobacteria, Oligoflexia and Gammaproteobacteria (Fig. 2).

Estimated species richness of individual colonies ranged from 2 to 74 non-*Microcystis* OTUs (Fig. S5). However, the majority of colonies had 10–40 non-*Microcystis* OTUs and a Shannon Index of 1.2–2.6 (a higher Shannon Index indicates a more diverse community in terms of species richness and evenness) and were less diverse than the communities in whole and 105 μm filtered water (Fig. S5). Mean colony species richness and diversity was highest in July and August (Fig. S6) and differed by *Microcystis* oligotype (Fig. S7). Phycosphere communities from oligotype 3 colonies had significantly greater estimated species richness and Shannon index than those of other *Microcystis* oligotypes, and oligotype 1 had higher richness and Shannon index than oligotype 2 on average (Fig. S7). There were no

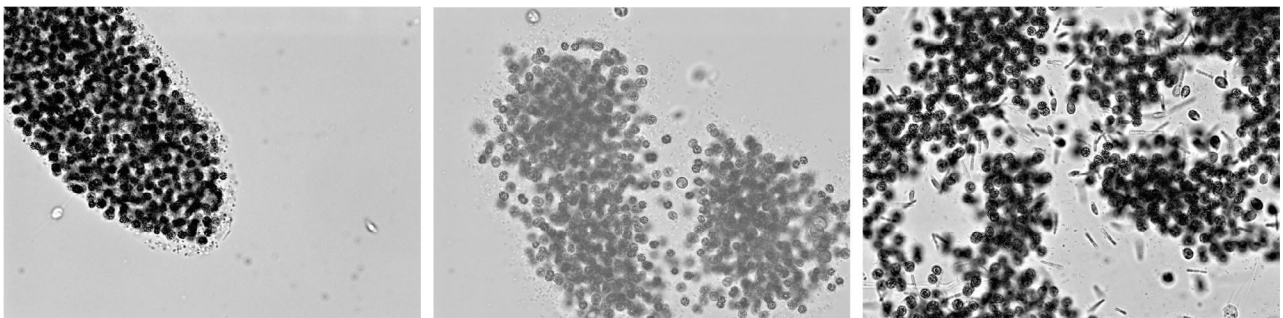


Fig. 1. Example black and white micrographs of *Microcystis* colonies in bulk phytoplankton seston collected from western Lake Erie blooms. The larger, dark cells are *Microcystis* cells, and the surrounding rod and cocci cells are the non-*Microcystis* cells that colonize the phycosphere.

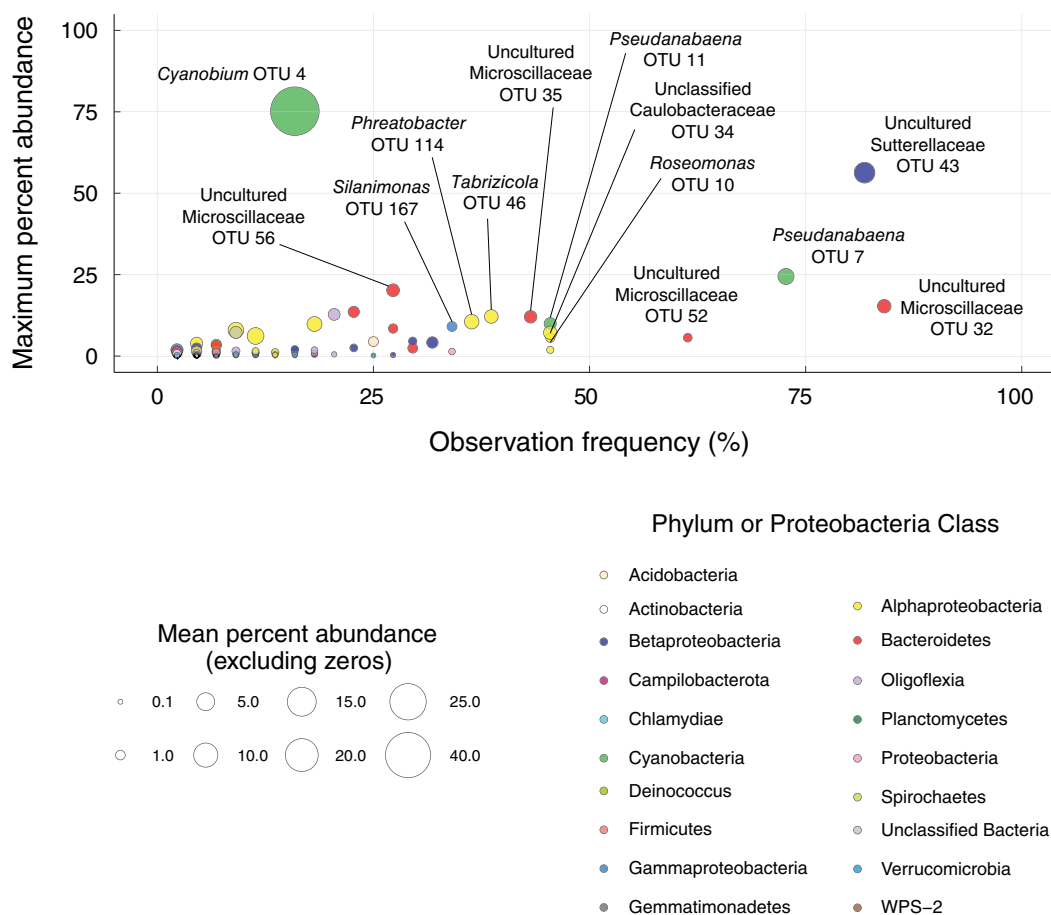


Fig. 2. Maximum and mean relative abundance of all non-*Microcystis* OTUs identified in the *Microcystis* phycosphere plotted against their observation frequency. Observation frequency was calculated as the percent of total colonies on which a given OTU was observed. Bubble size is scaled to mean relative abundance of the OTU in colonies where it was present. Bubble colour represents the OTU phylum (or class in the case of Proteobacteria). [Color figure can be viewed at wileyonlinelibrary.com]

significant correlations between species richness or Shannon index and colony size (Fig. S8).

Microcystis phycosphere communities are dissimilar from bulk community samples

To compare *Microcystis* phycosphere communities with surrounding communities, we performed hierarchical clustering (HC) and ordination of the colony-associated sequences together with those from whole water, 105 μm filtered samples, and bulk 100 μm retentate from western Lake Erie CHAB communities in 2014 and 2017–2019. HC and non-metric multidimensional scaling (NMDS) yielded four clearly separated main clusters (Fig. 3): one containing all the bulk 100 μm retentate samples from 2014 (cluster A), another containing *Microcystis* colonies dominated by *Cyanobium* (cluster B), another containing all whole and 105 μm filtered water samples (cluster C), and another containing all the remaining individual *Microcystis* colonies (cluster D). This clustering is supported

by the results of an ANOSIM test, which showed statistically significant differences in mean community dissimilarity between the HC groups ($R = 0.9787$, $P = 1 \times 10^{-5}$). Whole water samples across the four sampling seasons clustered together by month collected (Fig. S9, ANOSIM $R = 0.3588$, $P = 1 \times 10^{-4}$) and chlorophyll *a* concentration (Fig. S10, Mantel test $\rho = 0.3967$, $P = 1 \times 10^{-4}$), suggesting that the whole water microbial communities in western Lake Erie are similar between years and change in a consistent manner both seasonally and as *Microcystis* blooms develop. Despite these shifts in bulk community composition, the dissimilarity within sample types (whole water, filter fraction, or individual colony) across all years was significantly lower than the dissimilarity across sample types (ANOSIM, $R = 0.7534$, $P = 1 \times 10^{-5}$) and indicates that the *Microcystis* phycosphere harbours a community of bacteria distinct from the total and free-living communities, as suggested previously in bulk cyanobacterial colony samples dominated by *Microcystis* (Parveen *et al.*, 2013;

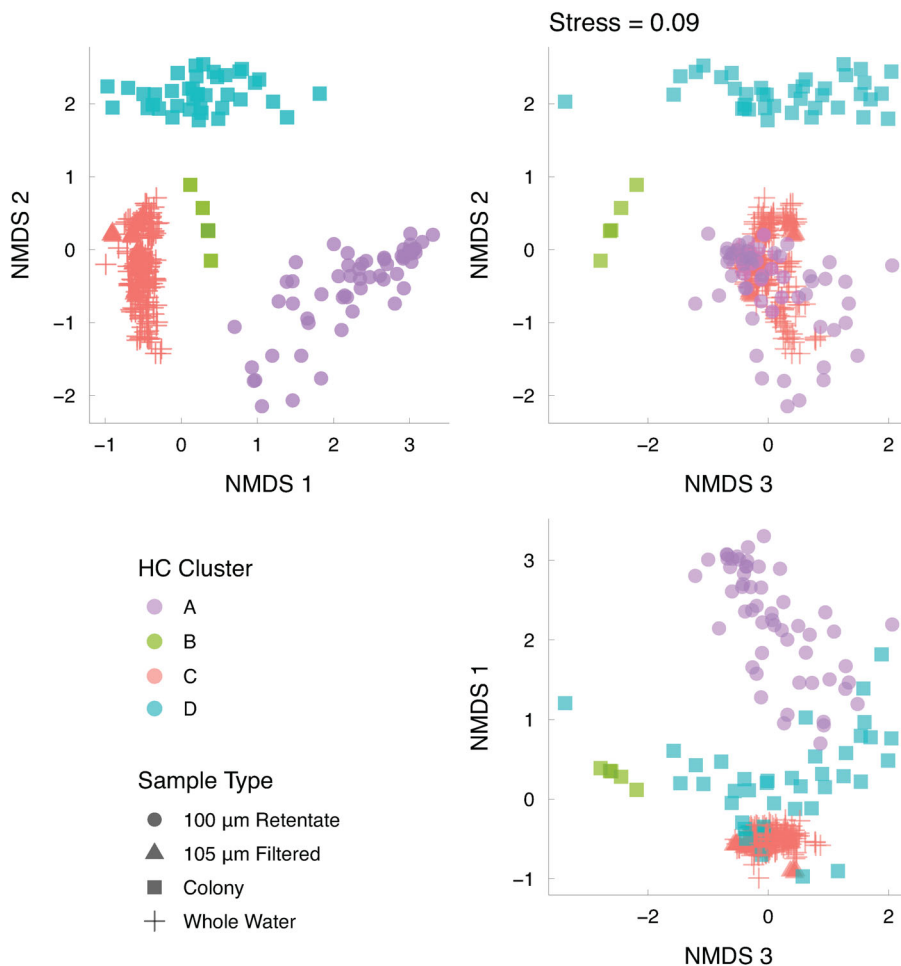


Fig. 3. NMDS ordination of bacterial communities in the *Microcystis* phycosphere, 100 µm retentate, 105 µm filtered, and whole water communities from western Lake Erie. The plot axes show NMDS scores. Points in the ordination are coloured by hierarchical clustering assignment. The point shapes in the ordination reflect sample type. [Color figure can be viewed at wileyonlinelibrary.com]

Louati *et al.*, 2015; Jankowiak and Gobler, 2020). In addition, high dissimilarity between single colony communities and bulk 100 µm retentate communities demonstrates that bacterial communities in bulk seston samples include communities associated with multiple phytoplankton and other particles that are not representative of *Microcystis* phycosphere communities. While the retentate samples were collected in a different year from the single *Microcystis* colonies, the lower dissimilarity within groups of the same sample type across multiple years supports that this comparison is robust, albeit imperfect. These results support the idea that the *Microcystis* phycosphere provides an ecologically distinct microenvironment, similar to the phycospheres of other algae (Hasegawa *et al.*, 2007; Burke *et al.*, 2011b) and cyanobacteria (Hmelo *et al.*, 2012; Zhu *et al.*, 2019). The distinct communities directly associated with *Microcystis* colonies versus those in the filter fraction dominated by *Microcystis* colonies (i.e., bulk 100 µm retentate) also shows that bacteria in the latter should not necessarily be considered physically associated with *Microcystis* and

may be attached to other phytoplankton or particles > 100 µm in size.

The Microcystis phycosphere lacks a core community

While the *Microcystis* phycosphere communities are more similar to each other than to whole water communities, there was high variation in phycosphere community composition. Dissimilarity was higher between *Microcystis* phycosphere communities than between whole water samples (Fig. S11). Consistent with this finding, only nine OTUs were conserved across all colonies of a specific date or oligotype (Table S2). The majority of non-*Microcystis* OTUs occurred infrequently, yet some could comprise a large proportion of the phycosphere community when present (Fig. 2, Table S3). A few OTUs occurred more frequently, and the top four most frequently observed non-*Microcystis* OTUs were present in 61%–84% of all *Microcystis* colonies sequenced ($n = 44$, Fig. 2, Table S4), suggesting that while these taxa are not universally present, they are more conserved taxa

across the phycospheres of multiple *Microcystis* strains. Supporting this interpretation, OTUs 7 and 11 (*Pseudanabaena*) and OTU 32 (uncultured Microscillaceae) were found at high relative abundance on multiple *Microcystis* oligotypes (Fig. 4). The observation of more conserved taxa across multiple strains is consistent with previously published results with bulk communities that identified a few bacterial taxa as regular members of the *Microcystis* phycosphere (Parveen *et al.*, 2013; Cook *et al.*, 2020; Jankowiak and Gobler, 2020).

Although some OTUs were frequently associated with *Microcystis* colonies, the relative abundance of all OTUs that were detected showed high variance across all colonies, as reflected in the difference between their maximum and mean relative abundances (Fig. 2). Furthermore,

no non-*Microcystis* OTUs were found in every colony (Fig. 2). The high variability in *Microcystis* phycosphere community composition contrasts with the phycosphere communities of other phytoplankton taxa, which have more stable core phycosphere communities (Frischkorn *et al.*, 2017; Lee *et al.*, 2017; Behringer *et al.*, 2018). However, high variation in the phycosphere communities of *Microcystis* has been previously observed (Shia *et al.*, 2010; Parveen *et al.*, 2013; Kim *et al.*, 2019; Jankowiak and Gobler, 2020), and the phycospheres of other phytoplankton can vary based on morphology (Hmelo *et al.*, 2012; Rouco *et al.*, 2016), strain (Jasti *et al.*, 2005; Sapp *et al.*, 2007; Ajani *et al.*, 2018; Jackrel *et al.*, 2019; Kim *et al.*, 2019), stage of growth (Sapp *et al.*, 2007), location (Rouco *et al.*, 2016; Ajani *et al.*, 2018; Kim *et al.*, 2019; Jankowiak and

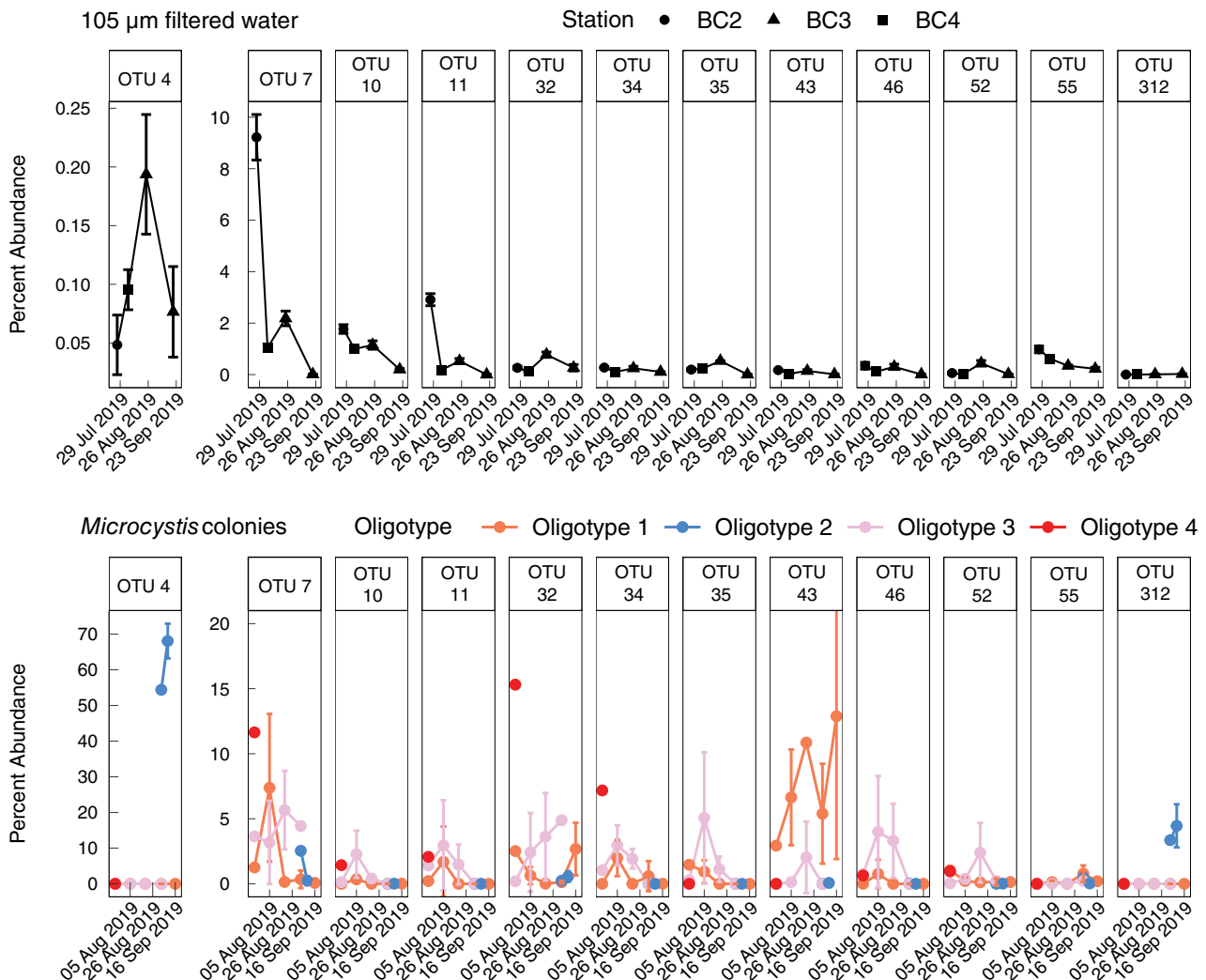


Fig. 4. Changes in the relative abundance of OTUs that are frequently present or indicators of date or *Microcystis* oligotype in *Microcystis* phycosphere communities. Mean relative abundances in both 105 µm filtered water samples from 2019 (top) and single *Microcystis* colonies (bottom) are shown. Error bars depict 95% confidence intervals. No error bars indicate that only one colony of the given oligotype was sampled on that particular date. [Color figure can be viewed at wileyonlinelibrary.com]

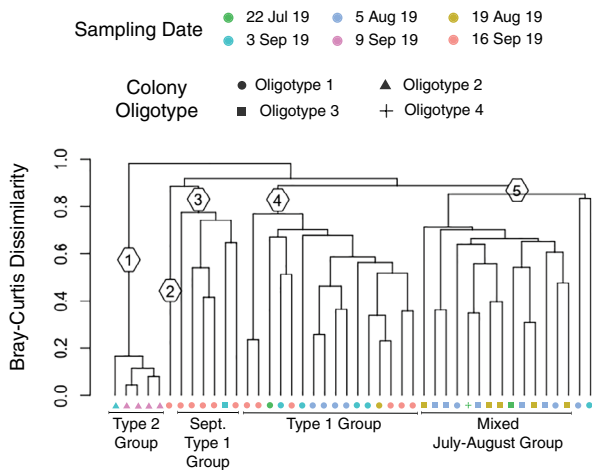


Fig. 5. Hierarchical clustering of bacterial communities in the *Microcystis* phycosphere. Branches in the dendrogram are numbered by hierarchical clustering assignments (shown as numbers in hexagons) based on Bray–Curtis dissimilarity. The shape and colour of the points at the leaves of the dendrogram indicate oligotype and sampling date, respectively, and match the corresponding point in the NMDS ordination (Fig. S12). [Color figure can be viewed at wileyonlinelibrary.com]

Gobler, 2020), and time of year (Jankowiak and Gobler, 2020). Our results from individual colonies suggest that few bacterial taxa are commonly associated with all *Microcystis* strains or inhabit the phycosphere throughout the growing season. Thus, *Microcystis* lacks a ‘core’ microbiome from a taxonomic perspective.

Microcystis phycosphere communities vary with time and *Microcystis* oligotype

To investigate drivers of the differences in *Microcystis* phycosphere community composition, we performed HC and NMDS ordination of *Microcystis* phycosphere communities alone. This analysis revealed that the *Microcystis* phycosphere communities could be assigned to five groups based on Bray–Curtis dissimilarity. Group membership is correlated with sampling date and oligotype as supported by an ANOSIM test, which revealed significant differences in mean colony dissimilarity by sampling date ($R = 0.4111$, $P = 1 \times 10^{-4}$) and *Microcystis* oligotype ($R = 0.4933$, $P = 1 \times 10^{-4}$, Figs 5 & Fig. S12). There was also a significant difference based on colony morphology, but the correlation coefficient was low ($R = 0.1974$, $P = 0.004$). Results using MED nodes were similar, showing significant correlations with sampling date ($R = 0.476$, $P = 1 \times 10^{-4}$) and oligotype ($R = 0.3747$, $P = 1 \times 10^{-4}$) that were similar in value to the results with OTUs, although the effect was stronger with date when using MED nodes. One HC cluster was comprised of a community from a single oligotype 1 colony (cluster 2), while the remaining four HC groups

included communities from multiple colonies (Fig. 5). In the following, we consider the evidence for oligotype and sampling date as drivers of phycosphere community composition, then discuss these results in the context of two hypotheses: (1) recruitment of the *Microcystis* microbiome is selective based on allelopathic or metabolic interactions, or (2) recruitment of the *Microcystis* microbiome is neutral or influenced by different ‘seeding communities’ in the surrounding water that change through time.

Microcystis oligotype appears to be a strong driver of community dissimilarity. Three of the four major groups identified with HC were comprised of communities from a single *Microcystis* oligotype (clusters 1, 3 and 4), with the exception of one colony in cluster 3 (Fig. 5). In addition, some abundant OTUs were primarily associated with a single *Microcystis* oligotype (Fig. 4). For example, OTU 43 (uncultured Sutterellaceae), OTU 4 (*Cyanobium*), and OTU 46 (*Tabrizicola*) were predominantly found on oligotype 1, oligotype 2, and oligotype 3 colonies, respectively (Fig. 4). This finding is consistent with previous studies that have shown that the abundance of certain bacterial OTUs during blooms are correlated with the abundance of specific *Microcystis* genotypes (Chun *et al.*, 2020). The clustering by colony oligotype suggests that different *Microcystis* strains harbour characteristic microbiomes.

There were also significant differences in phycosphere communities by sampling date. Two of the HC clusters (clusters 1 and 3) were comprised of primarily one sampling date. Three clusters were comprised primarily of colonies collected within a single month; clusters 1 and 3 were comprised entirely of colonies collected in September. Cluster 5 was comprised of colonies from July and August, with the exception of one colony that was collected in September (Fig. 5). The two most frequently observed *Microcystis* MED nodes in the colonies (nodes 8432 and 8437) were present in whole water samples at comparable abundance, and both of these MED nodes were most abundant in July–August and decreased in September (Fig. S4). In addition, *Microcystis* node 1993 was present at very low abundance in bulk community samples at all time points. These trends in *Microcystis* node abundance support that the effect of time cannot be attributed to an autocorrelation with shifts in *Microcystis* MED node abundance in bulk community samples. Further supporting this, colonies in cluster 5 were all collected in July and August yet spanned multiple oligotypes (although the majority were from oligotype 3, Fig. 5). These clustering patterns suggest that temporal effects play a role in driving phycosphere community dissimilarity. However, with our data, we cannot rule out the possibility that the significant clustering by time is due to shifts in the abundance of *Microcystis* strains that are

not differentiated with 16S V4 oligotypes. In addition, because cluster 1 contained all of the oligotype 2 colonies and mostly colonies collected from 9 September 2019, and oligotype 3 colonies were mostly sampled in August (Fig. 2B), it is difficult to interpret whether the significant differences in the phycosphere community composition of these colonies is due to sampling date or *Microcystis* oligotype (Fig. 5). Overall, the currently available data are not sufficient to determine the relative influence of colony oligotype and sampling date on *Microcystis* phycosphere community composition.

Of the HC clusters that separated by *Microcystis* oligotype, cluster 1 included all the samples from station WE16 (Fig. 5, station WE16 was sampled on 9 September 2019). While this cluster was not exclusive to colonies from station WE16, the predominance of colonies from station WE16 could indicate that differences in this cluster are driven by spatial differences in bacterial communities rather than by differences in date or *Microcystis* oligotype. However, the dissimilarity in whole water communities from multiple nearshore sites in the lake were low (Fig. 3), and a previous study showed that microbial communities in western Lake Erie vary more seasonally than spatially (Berry *et al.*, 2017a). Therefore, it is unlikely that cluster 1 is an effect of station rather than *Microcystis* oligotype or time.

Potential mechanisms to explain the degree of clustering by Microcystis oligotype

Several mechanisms could feasibly explain a strain-dependence in *Microcystis* phycosphere community composition. Different *Microcystis* strains may release distinct antibiotics that inhibit the growth of various bacterial taxa in the phycosphere differently. Production of antibiotic compounds has been observed in *Microcystis* (Casamatta and Wickstrom, 2000) and other phytoplankton (Ribalet *et al.*, 2008). Likewise, given that many bacteria are able to colonize the phycosphere via chemotaxis (Bell and Mitchell, 1972; Paerl and Gallucci, 1985; Sonnenschein *et al.*, 2012; Raina *et al.*, 2019) to specific types of organic compounds (Bell and Mitchell, 1972; Bassler *et al.*, 1991; Casamatta and Wickstrom, 2000; Miller *et al.*, 2004; Seymour *et al.*, 2010), different *Microcystis* strains may excrete a unique pool of organic molecules that attract different heterotroph populations. Differences in the production of secondary metabolites (Le Manach *et al.*, 2019) and the sugar composition of exopolysaccharides (Forni *et al.*, 1997) have been observed between *Microcystis* strains and species, suggesting that metabolites in the phycospheres of different strains vary. Similarly, the production and consumption of metabolites by the bacteria that colonize the phycosphere may also impact the chemotaxis of other bacterial populations. For example,

Cyanobium, *Pseudanabeana*, uncultured Sutterellaceae, and uncultured Microscillaceae likely play a major role in uptake and production of metabolites in the *Microcystis* phycosphere due to their high relative abundance in the colonies on which they were present (Fig. 2). To our knowledge, the composition and structure of DOC in the *Microcystis* phycosphere has not been fully characterized. Future studies that identify the organic compounds that are in the phycosphere and transferred among community members, characterize the ability of different excreted DOC molecules to attract chemotactic bacteria, and determine how excreted DOC varies between different *Microcystis* strains are required to describe the mechanism of how different strains of *Microcystis* harbour distinct phycosphere communities.

Despite significant clustering by *Microcystis* oligotype, there was also substantial dissimilarity between phycosphere communities that shared a colony oligotype. For example, oligotype 1 colony communities were separated into two main HC clusters (clusters 3 and 4, Fig. 5). The Bray–Curtis dissimilarity between these groups was > 0.8 and could be > 0.6 within the groups (Fig. 5). The effect of sampling date alone is unlikely to explain the differences between clusters 3 and 4 because cluster 4 included colonies from a range of different sampling dates, and both clusters contained colonies from September. The high dissimilarity within and between HC groups that share an oligotype and sampling dates suggests that *Microcystis* oligotype and date alone are insufficient to describe all of the dissimilarity in phycosphere community composition.

Dissimilarity in phycosphere communities between colonies that share an oligotype and sampling date could be explained by unresolved *Microcystis* strain differences, or by neutral effects. Because *Microcystis* 16S oligotypes are paraphyletic (Berry *et al.*, 2017b), colonies of the same oligotype may not necessarily be similar strains. Therefore, distinct HC clusters of primarily the same *Microcystis* oligotype may reflect microbiomes of *Microcystis* strains that share a 16S oligotype but vary in other traits that determine phycosphere community composition. Alternatively, neutral processes such as the random colonization of the phycosphere could explain the differences in phycosphere communities from colonies of the same oligotype. Neutral processes were hypothesized as the primary determinant of community composition in epiphytic communities of macroalgae (Burke *et al.*, 2011b). Indeed, the lack of a core microbiome and the low number of consistently present taxa in *Microcystis* phycosphere communities is similar to the epiphytic communities of macroalgae (Burke *et al.*, 2011b). Random colonization of distinct niches within the phycosphere by specific bacterial groups with similar ecologies, referred to as the ‘lottery hypothesis’ (Burke

et al., 2011a; Burke et al., 2011b), may reconcile the significant clustering by both time and oligotype and the high phycosphere community dissimilarity between colonies of the same oligotype. The lottery hypothesis requires functional redundancy across the potential colonizing species (Burke et al., 2011a), which has been observed in taxonomically different bacterial communities in *Microcystis* dominated bulk seston (Cook et al., 2020) and *Microcystis* enrichment cultures (Jackrel et al., 2019). However, the significant clustering by date and oligotype (Fig. 5 & Fig. S12), and the consistent patterns in the abundance of certain OTUs with time and *Microcystis* oligotype (Fig. 4) conflict with the hypothesis that random colonization is a major determinant of *Microcystis* phycosphere community composition and rather suggest that selective mechanisms have a role in determining the differences in *Microcystis* phycosphere community composition, at least in part. The idea that selective mechanisms determine *Microcystis* phycosphere community composition is congruent with previous observations in that phytoplankton cultures of the same genus or species have more similar associated bacteria communities than those from other phytoplankton taxa (Grossart et al., 2005; Jasti et al., 2005; Sapp et al., 2007; Bagatini et al., 2014; Behringer et al., 2018), and bacteria colonize diatom cultures in a predictable manner (Mönnich et al., 2020). Ultimately, future datasets with better resolution of *Microcystis* strains, along with colonization experiments using different *Microcystis* strains and bacterial inocula, are required to determine the relative importance of selective and neutral processes in shaping *Microcystis* phycosphere community composition.

Potential mechanisms to explain clustering by sampling date

Our results provide evidence that shifts in seeding communities from the surrounding water may have a significant role in shaping phycosphere community structure. Supporting this hypothesis, several OTUs (OTU 7 *Pseudanabaena*, OTU 10 *Roseomonas*, OTU 11 *Pseudanabaena*, OTU 34 *Caulobacteraceae*) that were present on multiple *Microcystis* oligotypes showed decreases in the average relative abundances of these OTUs on the colonies that corresponded with decreases in their average relative abundance in 105 µm filtered water (Fig. 4). This observation is consistent with previous work showing that inoculum source had a significant impact on bacterial community composition in a *Microcystis* culture colonization experiment (Dziallas and Grossart, 2011), and that the composition of bacterial communities in western Lake Erie show strong seasonal shifts (Berry et al., 2017a). Therefore, shifts in the

dominant members of chemotactic populations that seed the phycosphere may change phycosphere community composition over time. However, other OTUs were either present on all dates (OTU 43 Sutterellaceae) or the abundance trends on *Microcystis* colonies are not similar to trends in abundance in 105 µm filtered water (OTU 46 *Tabrizicola*, Fig. 4), which suggests that shifts in seeding communities may impact the abundances of only some phycosphere taxa.

Phenotypic differences based on changes in physiological state may impact the *Microcystis* phycosphere, as previously observed in other phytoplankton (Bell and Mitchell, 1972; Sapp et al., 2007). Indeed, *Microcystis* produces different classes and amounts of DOC at different growth phases, growth rates, and temperature and nutrient regimes (Dziallas and Grossart, 2012; Li et al., 2013; Xu et al., 2013), which may serve as chemoattractants for different bacterial populations. The decline in both bulk phycocyanin and bulk chlorophyll a concentration in September (Fig. S2) indicates that a change in physiological state due to bloom termination could explain differences in the phycosphere communities collected at this time (Fig. 5). Larger data sets across multiple years with better resolution of *Microcystis* genotypes along with studies of how *Microcystis* metabolite excretion changes with physiological state are required to determine the relative importance of phenotypic changes across bloom development or growth stages on *Microcystis* phycosphere community composition.

Finally, we evaluated the potential influence of the physicochemical environment on phycosphere community composition. Mantel tests revealed that most environmental parameters (and combinations thereof) did not have a strong, significant correlation to phycosphere community dissimilarity. The exceptions were chromophoric dissolved organic matter (CDOM) absorbance (a proxy for CDOM concentration), depth-integrated PAR (surface – 0.5 m), nitrate concentration, and temperature (Table S5). However, linear regression models of community dissimilarity versus Euclidean distances of each environmental parameter had poor fits to the data ($R^2 < 0.1$ for all parameters, Fig. S13). Furthermore, there is high dissimilarity between colonies collected on the same date and location (Fig. 5), which would have experienced the same bulk water chemistry. Therefore, differences in the measured environmental parameters of the surrounding water cannot explain *Microcystis* phycosphere dissimilarity. However, changes in bulk DOC and nutrient concentrations relative to concentrations in the phycosphere may alter phycosphere community composition because the chemotactic response of heterotrophic bacteria is reduced under lower concentration

gradients of chemoattractants (Paerl and Gallucci, 1985; Bassler *et al.*, 1991).

Interactions between cyanobacteria in the phycosphere

In addition to non-cyanobacteria, the phycosphere communities included two *Pseudanabaena* OTUs and one *Cyanobium* OTU highly similar to an OTU classified as *Synechococcus* in a previous western Lake Erie study (Berry *et al.*, 2017a), that occurred at high relative abundance whenever present (Fig. 2). While *Cyanobium* dominated the colonies in which it occurred, micrograph images showed that *Microcystis* cells still made up the inner structure of those colonies and comprised a high percentage of the total colony communities (19.9% – 38.6%). While both cyanobacterial genera have been observed in *Microcystis* blooms (Ouellette *et al.*, 2006; Berry *et al.*, 2017a; Chun *et al.*, 2019; Chun *et al.*, 2020), only interactions between *Pseudanabaena* and *Microcystis* have been studied to our knowledge (Agha *et al.*, 2016; Zhang *et al.*, 2020). We note that *Cyanobium* was only observed in colonies collected on two dates, and single *Microcystis* cells were present in the droplets containing these colonies on one date (Fig. S14). We interpreted the stray *Microcystis* cells as breaking off colonies, and because *Cyanobium* is known to form aggregates by itself (Jezberová and Komárková, 2007), we cannot rule out that the *Cyanobium* in these samples are contaminants from broken *Cyanobium* colonies. However, other picocyanobacteria like *Cyanobium* were previously observed growing attached to *Microcystis* colonies (Hindák, 1996), so their association with *Microcystis* here likely reflects a true interaction within the phycosphere. The association of cyanobacteria within the *Microcystis* phycosphere is intriguing because it indicates that colonization of the phycosphere is not driven solely by a need for organic carbon to fuel respiration. It may indicate that *Pseudanabaena* and *Cyanobium* adhere to *Microcystis* colonies in order to obtain organic compounds (either from *Microcystis* or other attached bacteria) for which they are auxotrophic, or to actively inhibit growth of *Microcystis* via allelopathic interactions. Indeed, allelopathic interactions between *Pseudanabaena* and *Microcystis* have been observed previously, although the harmful effects on growth were limited to certain *Microcystis* strains (Agha *et al.*, 2016). Our data also suggests that such auxotrophic or allelopathic interactions between *Microcystis* and other cyanobacteria may be specific to certain *Microcystis* strains, as *Cyanobium* OTUs were specific to oligotype 2 colonies (Fig. 4, Table S3). Further characterization of the nature of the interactions between cyanobacteria genera in *Microcystis* colonies is required to fully understand their significance to *Microcystis* physiology.

Conclusion

This study found that bacterial communities in the *Microcystis* phycosphere of individual *Microcystis* colonies vary both with time and *Microcystis* oligotype and are distinct from communities in surrounding lake water as well as 100 µm community assemblages. Although *Microcystis* harbours a distinct microbiome in which certain bacterial taxa are commonly present and abundant, the absence of universal members of these communities indicates that there is no core *Microcystis* microbiome from a taxonomic perspective. The mechanism behind associations of *Microcystis* phycosphere community composition with time and oligotype are uncertain, but our data suggest that both selective and neutral processes are likely involved. The link of *Microcystis* phycosphere community composition to time and *Microcystis* oligotype suggest that interactions in the phycosphere may differentially impact specific *Microcystis* strains at different times. The impacts bacteria have on the growth of *Microcystis* (Agha *et al.*, 2016; Schmidt *et al.*, 2020) and other phytoplankton taxa (Sison-Mangus *et al.*, 2014; Amin *et al.*, 2015) vary depending on the phytoplankton strain. Therefore, the taxa occupying the phycosphere could influence competition between *Microcystis* strains through their different impacts on *Microcystis* growth, which may in turn change *Microcystis* strain composition in blooms and influence bloom development and toxin production. However, recent studies found that phycosphere communities of *Microcystis* enrichment cultures (Jackrel *et al.*, 2019) and bulk cyanobacteria colonies (Cook *et al.*, 2020) that were taxonomically distinct between strains had similar functional potential. Therefore, the extent to which phycosphere communities yield different outcomes on *Microcystis* growth and physiology remains unclear. Additionally, further investigation is needed to better understand how changes in phycosphere community composition of individual colonies interact with surrounding physicochemical conditions and free-living heterotrophic bacteria communities to influence *Microcystis* bloom development and toxin production. These results highlight the crucial need to characterize the interactions that take place between *Microcystis* spp. and their phycosphere communities and determine how they influence *Microcystis* biology and bloom development.

Experimental procedures

Field sampling

Microcystis colonies were collected approximately biweekly at two locations in western Lake Erie (Fig. S1) during the 2019 CHAB. The majority of colonies were sampled from NOAA station WE8, with the exception of

one date (9 September 2019), on which station WE16 was sampled. Sample collection covered a range of bloom development stages and microcystin concentrations (Fig. S2). *Microcystis* biomass was collected with 2–4 casts of a 53 μm plankton net, which retains 99% of *Microcystis* cells (Chaffin *et al.*, 2011). Biomass retained on the net was backwashed into 1–2 50 ml centrifuge tubes with 0.22 μm filtered and autoclaved Lake Erie water. The collected material was stored in a cooler filled with lake water until arrival back at the lab. Between each cruise, the plankton net was disinfected with 10% bleach and rinsed with DI water. Environmental and water chemistry data were obtained from NOAA's National Centres for Environmental Information (accession 0209116).

Individual colony isolation via droplet encapsulation

Immediately upon arrival to the lab, the biomass was filtered through a 300 μm pore size filter mesh and retained on filter mesh with 105 μm pore size. The 105 μm retentate from all samples collected on a given date were transferred to a new 50 ml falcon tube using a squirt bottle containing molecular grade PBS. Then, the falcon tube was filled to 30 ml with molecular grade PBS. The biomass was allowed to settle for 10 min, which caused non-cyanobacterial particles to sink and cyanobacteria colonies to buoyantly float to the top of the solution (Shi *et al.*, 2018; Zhu *et al.*, 2019). The buoyant colonies were then transferred to a new falcon tube using a sterile pipette and resuspended in new molecular grade PBS solution. This colony wash and transfer was repeated five additional times to separate loosely attached or free-living bacteria from the colonies. On the final washing step, the colonies were collected and placed into a sterile 2 ml microcentrifuge tube. The concentration of colonies was estimated by dispensing 5 μl aliquots onto multiple glass slides and counting colonies under an inverted light microscope.

After washing, droplet encapsulation of the cyanobacterial colonies was performed using a syringe pump to encapsulate the colony suspension into droplets that could be individually processed (Fig. 6). First, the cyanobacterial colonies were diluted to approximately 67 colonies ml^{-1} (one colony in every 15 μl) with PBS solution and loaded into a 10 ml luer-lock syringe with a 23 gauge needle (337 μm inner diameter), along with 1 ml of air. The syringe was loaded into a syringe pump (Kent Scientific, GenieTouch™) set to a continuous flow rate of 600 $\mu\text{l min}^{-1}$ and placed on top of an orbital shaker set to 100–150 rpm (Fig. 6). Tubing (PTFE, 0.022x0.042", Cole-Parmer EW-06417-21) attached to the syringe needle allowed a droplet (~15 μl volume) to form and fall onto a section of a sterile petri dish. Before droplets were formed with the colony suspension,

several droplets were formed with sterile PBS solution to serve as blank controls for subsequent sequencing. All droplets were inspected and imaged with an inverted light microscope (Nikon Eclipse Ti-S). Droplets containing one *Microcystis* colony were transferred to a 96 well PCR plate using a P1000 micropipette tip. The larger volume tip was required to prevent the colonies from adhering to the tip. The PCR plate was covered with sterile aluminium foil (VWR 89049-034) and frozen at -20°C until DNA extraction. In total, we screened 800 droplets and collected 210 droplets that contained a single *Microcystis* colony.

Colony dimensions were measured from microscopy images with ImageJ (2.0.0-rc-69/1.52i). Length and width were defined by drawing lines through the longest and shortest dimensions, respectively, on 2D colony images. Area was drawn by manual free-hand selection around the distinguishable boundary of the colony. The scale ($\mu\text{m}/\text{pixel}$) was calculated using scale bars from microscopy. Colony morphology was assigned using published morphospecies classifications (Otsuka *et al.*, 2000).

DNA extraction and sequencing

DNA extractions of colonies and PBS blanks were performed with ChargeSwitch® gDNA Mini Bacteria Kits (Invitrogen Life Technologies, California, USA) using a protocol modified for single *Microcystis* colonies (Pérez-Carrascal *et al.*, 2019). From the 210 droplets collected, DNA was extracted from 122 colonies (17–25 for each sampling date) in a laminar flow-hood to minimize contamination from the lab. Because single colony samples had very low biomass, the samples were subjected to a round of PCR using dual indexed primers targeting the V4 region of the bacterial 16S rRNA gene (Kozich *et al.*, 2013) to confirm the presence of amplifiable DNA in the samples and its absence in PBS blanks. The raw DNA extracts of blanks and all amplifiable samples ($n = 60$) were submitted for sequencing using Illumina MiSeq V2 500 cycle chemistry (Illumina cat# MS102-2003) at the University of Michigan Microbial Community Analysis Core following their SOP (Schloss and Bishop, 2019).

DNA collected from microbial communities in whole and 105 μm filtered water from western Lake Erie in the summer and fall of 2014 and 2017–2019 was compared to phycosphere communities. Amplicon data from the 2014 bloom was obtained from a previously published study (Berry *et al.*, 2017a). Whole water microbial communities from 2017–2019 were collected by filtering 100–200 ml of lake water through a 0.22 μm PES filter. The filter was preserved in RNeasy and frozen at -80°C until DNA extraction. Microbial communities from the < 105 μm size fraction (smaller than the *Microcystis*

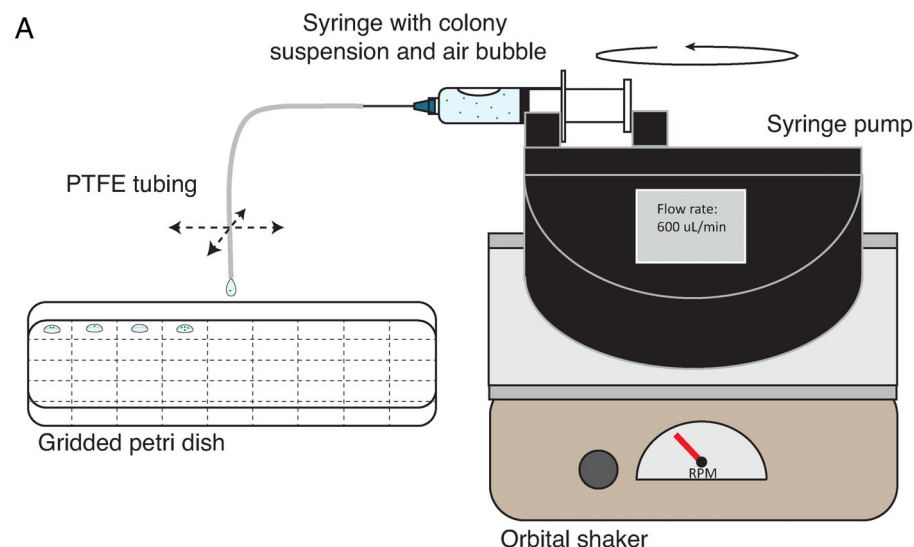


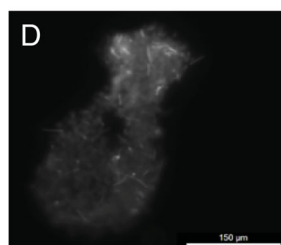
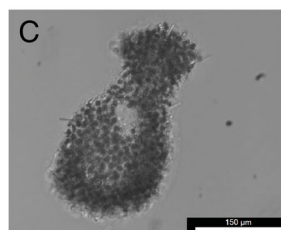
Fig. 6. Description of droplet encapsulation method.

A. Encapsulation of *Microcystis* colonies into droplets with a syringe-pump on an orbital shaker. The colony suspension flowed out of the syringe into the tubing at a constant rate of 600 µL min⁻¹. A homogeneous suspension of buoyant colonies was maintained through the jostling of the air bubble in the syringe using the orbital shaker (100–150 rpm). Tubing was manually moved so that droplets were dispensed onto number sections of a sterile petri dish. Each droplet was then examined with an inverted light microscope.

B. Example micrograph image of a droplet containing one *Microcystis* colony.

C. Higher-resolution image of the colony in *b*.

D. Image of the colony in *c* shown with phycocyanin autofluorescence. [Color figure can be viewed at wileyonlinelibrary.com]



colonies sequenced) were collected by filtering whole lake water through a 105 µm plankton mesh and collecting the filtrate into an acid-washed 2 l polycarbonate bottle. Then, 200 ml of the 105 µm filtrate was filtered through a 0.22 µm PES filter, preserved in RNAlater and frozen at -80°C until DNA extraction. In 2017, filters were collected weekly at NOAA monitoring station WE2 and periodically near the drinking water intake for Toledo, OH, and at various Environment Canada monitoring sites during two research cruises (Fig. S1). Filters were collected during pre-bloom, early bloom, mid bloom, and late bloom phases from NOAA station WE2 and the drinking water intake for Toledo, OH in 2018, and at locations of highest bloom density as predicted by the NOAA HAB tracker in 2019 (Wynne *et al.*, 2013). The water used for total microbial communities in 2017–2019 was stored for 12–15 h in carboys placed in an outdoor water bath

set to lake water temperature before sample collection. DNA was extracted from the filters using QIAGEN DNeasy Blood & Tissue Kits with QIAshredder columns (QIAGEN, Maryland, USA). Genomic DNA from *Thermus thermophilus* strain DSM 7039 was added to the samples after the cell lysis step of the extraction as an internal standard. *Thermus thermophilus* DNA was obtained from the American Type Culture Collection (ATCC; product number BAA-163D-5). The internal standard was added as ~1% of DNA yield, which was estimated based on an empirically determined relationship between total mass of chlorophyll *a* on the filter and DNA yield. DNA yields were measured with Quant-iT Picogreen dsDNA Assay Kit (Invitrogen, Carlsbad, CA). The true percentage of the internal standard was 0.72 ± 0.37% of total DNA yield on average. The extraction protocol is included as a supplemental data file.

Bioinformatic and statistical analyses

Forward and reverse reads were quality screened to remove sequences below 250 bases and trimmed to Q20 using BBDuk (Bushnell, 2014). Any read pairs in which a read had 50% or more of the bases trimmed were removed from downstream analysis. Any samples that had fewer than 1000 reads after QC were not included in downstream analysis (final $n = 44$). Following trimming, overlapping forward and reverse reads were assembled into contigs, aligned, screened for chimeras, and clustered into OTUs using MOTHUR v. 1.43.0, following the SOP as of February 2020 (Kozich *et al.*, 2013). OTU clustering was performed using a 97% similarity cutoff with the OptiClust algorithm (Westcott and Schloss, 2017). Contigs were aligned with the align.seqs function in MOTHUR, and taxonomy was assigned using the Wang method (Wang *et al.*, 2007). Silva v. 138 SSU database (Pruesse *et al.*, 2007) was used as the reference to align and classify the contigs. The data were also clustered into oligotype OTUs (referred to as nodes in the original paper) using minimum entropy decomposition (MED) without outlier replacement (Eren *et al.*, 2015). The minimum substantial abundance at which an MED node was reported was set to 854, following the previously published suggestion of using $N/10\ 000$, where N is the total number of sequences in the dataset (Eren *et al.*, 2015). The relative abundance of the 97% OTUs and MED nodes in each sample was calculated as the proportion of the total reads from a sample that were assigned to a given OTU or MED node. MED nodes were used to resolve finer-scale variation in *Microcystis* sequences, and 97% OTUs were used for overall comparisons of non-*Microcystis* community composition to avoid confounding effects of sequence variation in MED nodes that may reflect nonidentical gene copies originating from a single genome rather than genes from different species. All OTUs classified as *Thermus* in bulk samples were removed from the dataset prior to NMDS analysis and relative abundance calculation. The absolute abundance of MED nodes in bulk community samples was calculated from the recovery of the internal standard following previously published methods (Lin *et al.*, 2019).

To determine the nucleotide similarity of multiple 16S rRNA gene copies in *Microcystis* genomes, 16S rRNA gene sequences were downloaded from each closed *Microcystis* genome available in NCBI (as of 24 June 2020; $n = 9$). Then the gene copies from each genome were aligned using the blastn function in the NCBI web tool. *Microcystis* colonies were assigned to oligotype groups based on the identity of their pairs of MED sequence variants (Oligotype 1 = Nodes 8432-8432, Oligotype 2 = Nodes 1993-8432, Oligotype 3 = Nodes 8437-8437, Oligotype 4 = Nodes 8432-8437).

Because interpretations of community structure in low biomass samples are significantly altered by contamination from the lab and DNA extraction kits (Salter *et al.*, 2014), we screened the final OTUs for contaminating taxa, following previously published suggestions (Salter *et al.*, 2014; Sheik *et al.*, 2018). First, all OTUs comprised of 1–2 sequences or present in only one colony at $\leq 0.1\%$ abundance were removed from the data set. Second, we checked the legitimacy of any OTUs in the *Microcystis* colonies classified with a taxonomy that matched to known contaminants from DNA extraction kits (Salter *et al.*, 2014; Sheik *et al.*, 2018) by screening for their presence in the field samples. Potential contaminant OTUs with a relative abundance that was significantly different from zero in all field samples were removed from the colony dataset. The taxonomic assignments of contaminant OTUs flagged for removal were confirmed by blasting the representative sequence against the NCBI nr database.

Alpha diversity metrics, Bray-Curtis dissimilarities between colonies, NMDS ordinations, mantel tests, and ANOSIM tests were computed using the R package Vegan v. 2.5-6 (Oksanen *et al.*, 2013). Bray-Curtis dissimilarity was used as the distance metric for all beta-diversity calculations. Euclidean distance was used to measure dissimilarity in environmental parameters. HC of samples by Bray-Curtis dissimilarity was performed using an average linkage algorithm. All calculations of beta-diversity were performed without including *Microcystis* OTUs. Diagnostic species (species that are statistical predictors for classes of sites or samples) of sample date and oligotype were identified by calculating a complete Indval.g metric for each OTU using the R package indicpecies v. 1.7.9 (Cáceres and Legendre, 2009). Correlation analyses and other standard calculations were calculated using base R. All plots were made with ggplot2 v. 3.2.1 (<https://cran.r-project.org/web/packages/ggplot2/index.html>). The code for the entire bioinformatic and statistical analysis pipeline is publicly available at (<https://github.com/Geo-omics/Characterizing-individual-Microcystis-colony-phycosphere-communities>). The raw sequence data is deposited in NCBI SRA under BioProjects PRJNA645738 and PRJNA646259.

Acknowledgements

We thank Colleen Yancey, Dack Stuart, Kent Baker, and Paul Den-Uyl for field sampling support, the NOAA Great Lakes Environmental Research Lab and the Cooperative Institute for Great Lakes Research for letting us sample alongside their HAB monitoring efforts, Robert Hein for bioinformatics support and server maintenance, and Sean Blanchard for assistance with formatting micrograph images. This work was supported by National Science Foundation

Grant OCE-1736629 and the Rackham Graduate School at the University of Michigan.

Author contributions

D. J. S. and M. A. P. conducted field sampling. D. J. S., J. Y. T., and X. N. L. developed the colony isolation method. J. Y. T. performed colony isolations and microscopy measurements. D. J. S. performed DNA extraction, PCR, bioinformatics analysis, and statistical analysis. D. J. S. drafted and compiled the manuscript. All authors revised the manuscript and developed the experimental design and scientific questions.

References

- Adachi, M., Kanno, T., Okamoto, R., Itakura, S., Yamaguchi, M., and Nishijima, T. (2003) Population structure of *Alexandrium* (Dinophyceae) cyst formation-promoting bacteria in Hiroshima Bay, Japan. *Appl Environ Microbiol* **69**: 6560–6568.
- Agha, R., del Mar Labrador, M., de los Ríos, A., and Quesada, A. (2016) Selectivity and detrimental effects of epiphytic *Pseudanabaena* on *Microcystis* colonies. *Hydrobiologia* **777**: 139–148. <https://link.springer.com/article/10.1007/s10750-016-2773-z>.
- Ajani, P.A., Kahlke, T., Siboni, N., Carney, R., Murray, S.A., and Seymour, J.R. (2018) The microbiome of the cosmopolitan diatom *Leptocylindrus* reveals significant spatial and temporal variability. *Front Microbiol* **9**: 2758.
- Amin, S.A., Green, D.H., Hart, M.C., Krüpper, F.C., Sunda, W.G., and Carrano, C.J. (2009) Photolysis of iron-siderophore chelates promotes bacterial-algal mutualism. *Proc Natl Acad Sci* **106**: 17071–17076. <https://doi.org/10.1073/pnas.0905512106>.
- Amin, S.A., Hmelo, L.R., van Tol, H.M., Durham, B.P., Carlson, L.T., Heal, K.R., et al. (2015) Interaction and signalling between a cosmopolitan phytoplankton and associated bacteria. *Nature* **522**: 98–101. <https://doi.org/10.1038/nature14488>.
- Arandia-Gorostidi, N., Weber, P.K., Alonso-Sáez, L., Morán, X.A.G., and Mayali, X. (2017) Elevated temperature increases carbon and nitrogen fluxes between phytoplankton and heterotrophic bacteria through physical attachment. *ISME J* **11**: 641–650.
- Azam, F., and Malfatti, F. (2007) Microbial structuring of marine ecosystems. *Nat Rev Microbiol* **5**: 782–791.
- Bagatini, I.L., Eiler, A., Bertilsson, S., Klaveness, D., Tessarolli, L.P., and Vieira, A.A.H. (2014) Host-specificity and dynamics in bacterial communities associated with bloom-forming freshwater phytoplankton. *PLoS One* **9**: e85950.
- Barbara, G.M., and Mitchell, J.G. (2003) Bacterial tracking of motile algae. *FEMS Microbiol Ecol* **44**: 79–87.
- Bassler, B.L., Gibbons, P., Yu, C., and Roseman, S. (1991) Chitin utilization by marine bacteria. Chemotaxis to chitin oligosaccharides by *Vibrio furnissii*. *J Biol Chem* **266**: 24268–24275.
- Basu, S., Gledhill, M., de Beer, D., Matondkar, S.P., and Shaked, Y. (2019) Colonies of marine cyanobacteria *Trichodesmium* interact with associated bacteria to acquire iron from dust. *Commun Biol* **2**: 1–8.
- Behringer, G., Ochsenkühn, M.A., Fei, C., Fanning, J., Koester, J.A., and Amin, S.A. (2018) Bacterial communities of diatoms display strong conservation across strains and time. *Front Microbiol* **9**: 659.
- Bell, W., and Mitchell, R. (1972) Chemotactic and growth responses of marine bacteria to algal extracellular products. *Biol Bull* **143**: 265–277.
- Berry, M.A., Davis, T.W., Cory, R.M., Duhaime, M.B., Johengen, T.H., Kling, G.W., et al. (2017a) Cyanobacterial harmful algal blooms are a biological disturbance to Western Lake Erie bacterial communities. *Environ Microbiol* **19**: 1149–1162.
- Berry, M.A., White, J.D., Davis, T.W., Jain, S., Johengen, T. H., Dick, G.J., et al. (2017b) Are oligotypes meaningful ecological and phylogenetic units? A case study of *Microcystis* in freshwater lakes. *Front Microbiol* **8**: 365.
- Burke, C., Steinberg, P., Rusch, D., Kjelleberg, S., and Thomas, T. (2011a) Bacterial community assembly based on functional genes rather than species. *Proc Natl Acad Sci* **108**: 14288–14293.
- Burke, C., Thomas, T., Lewis, M., Steinberg, P., and Kjelleberg, S. (2011b) Composition, uniqueness and variability of the epiphytic bacterial community of the green alga *Ulva australis*. *ISME J* **5**: 590–600.
- Bushnell, B. (2014). *BBTools: A Suite of Fast, Multithreaded Bioinformatics Tools Designed for Analysis of DNA and RNA Sequence Data: Joint Genome Institute*. <https://jgi.doe.gov/data-and-tools/bbtools/>
- Cáceres, M.D., and Legendre, P. (2009) Associations between species and groups of sites: indices and statistical inference. *Ecology* **90**: 3566–3574.
- Casamatta, D., and Wickstrom, C. (2000) Sensitivity of two disjunct bacterioplankton communities to exudates from the cyanobacterium *Microcystis aeruginosa* Kütz. *Microb Ecol* **40**: 64–73.
- Chaffin, J.D., Bridgeman, T.B., Heckathorn, S.A., and Mishra, S. (2011) Assessment of *Microcystis* growth rate potential and nutrient status across a trophic gradient in western Lake Erie. *J Great Lakes Res* **37**: 92–100.
- Christie-Oleza, J.A., Sousoni, D., Lloyd, M., Armengaud, J., and Scanlan, D.J. (2017) Nutrient recycling facilitates long-term stability of marine microbial phototroph-heterotroph interactions. *Nat Microbiol* **2**: 1–10.
- Chun, S.-J., Cui, Y., Lee, C.S., Cho, A.R., Baek, K., Choi, A., et al. (2019) Characterization of distinct cyanoHABs-related modules in microbial recurrent association network. *Front Microbiol* **10**: 1637.
- Chun, S.-J., Cui, Y., Lee, J.J., Choi, I.-C., Oh, H.-M., and Ahn, C.-Y. (2020) Network analysis reveals succession of *Microcystis* genotypes accompanying distinctive microbial modules with recurrent patterns. *Water Res* **170**: 115326.
- Cole, J.J. (1982) Interactions between bacteria and algae in aquatic ecosystems. *Annu Rev Ecol Syst* **13**: 291–314.
- Cook, K.V., Li, C., Cai, H., Krumholz, L.R., Hambright, K.D., Paerl, H.W., et al. (2020) The global *Microcystis* interactome. *Limnol Oceanogr* **65**: S194–S207. <https://doi.org/10.1002/lno.11361>.

- Croft, M.T., Lawrence, A.D., Raux-Deery, E., Warren, M.J., and Smith, A.G. (2005) Algae acquire vitamin B₁₂ through a symbiotic relationship with bacteria. *Nature* **438**: 90–93. <https://doi.org/10.1038/nature04056>.
- Davis, T.W., Berry, D.L., Boyer, G.L., and Gobler, C.J. (2009) The effects of temperature and nutrients on the growth and dynamics of toxic and non-toxic strains of *Microcystis* during cyanobacteria blooms. *Harmful Algae* **8**: 715–725.
- Davis, T.W., Harke, M.J., Marcoval, M.A., Goleski, J., Orano-Dawson, C., Berry, D.L., and Gobler, C.J. (2010) Effects of nitrogenous compounds and phosphorus on the growth of toxic and non-toxic strains of *Microcystis* during cyanobacterial blooms. *Aquat Microb Ecol* **61**: 149–162.
- Durham, B.P., Dearth, S.P., Sharma, S., Amin, S.A., Smith, C.B., Campagna, S.R., et al. (2017) Recognition cascade and metabolite transfer in a marine bacteria-phytoplankton model system. *Environ Microbiol* **19**: 3500–3513. <https://doi.org/10.1111/1462-2920.13834>.
- Durham, B.P., Sharma, S., Luo, H., Smith, C.B., Amin, S.A., Bender, S.J., et al. (2015) Cryptic carbon and sulfur cycling between surface ocean plankton. *Proc Natl Acad Sci* **112**: 453–457.
- Dziallas, C., and Grossart, H.-P. (2011) Temperature and biotic factors influence bacterial communities associated with the cyanobacterium *Microcystis* sp. *Environ Microbiol* **13**: 1632–1641.
- Dziallas, C., and Grossart, H.-P. (2012) Microbial interactions with the cyanobacterium *Microcystis aeruginosa* and their dependence on temperature. *Mar Biol* **159**: 2389–2398.
- Eren, A.M., Borisy, G.G., Huse, S.M., and Welch, J.L.M. (2014) Oligotyping analysis of the human oral microbiome. *Proc Natl Acad Sci* **111**: E2875–E2884.
- Eren, A.M., Maignien, L., Sul, W.J., Murphy, L.G., Grim, S.L., Morrison, H.G., and Sogin, M.L. (2013) Oligotyping: differentiating between closely related microbial taxa using 16S rRNA gene data. *Methods Ecol Evol* **4**: 1111–1119.
- Eren, A.M., Morrison, H.G., Lescault, P.J., Reveillaud, J., Vineis, J.H., and Sogin, M.L. (2015) Minimum entropy decomposition: unsupervised oligotyping for sensitive partitioning of high-throughput marker gene sequences. *ISME J* **9**: 968–979.
- Ferrier, M., Martin, J., and Rooney-Varga, J. (2002) Stimulation of *Alexandrium fundyense* growth by bacterial assemblages from the bay of Fundy. *J Appl Microbiol* **92**: 706–716.
- Forni, C., Telo', F.R., and Caiola, M.G. (1997) Comparative analysis of the polysaccharides produced by different species of *Microcystis* (Chroococcales, Cyanophyta). *Phycologia* **36**: 181–185.
- Frischkorn, K.R., Rouco, M., Van Mooy, B.A., and Dyhrman, S.T. (2017) Epibionts dominate metabolic functional potential of *Trichodesmium* colonies from the oligotrophic ocean. *ISME J* **11**: 2090–2101.
- Grossart, H.P., Levold, F., Allgaier, M., Simon, M., and Brinkhoff, T. (2005) Marine diatom species harbour distinct bacterial communities. *Environ Microbiol* **7**: 860–873.
- Harke, M.J., Steffen, M.M., Gobler, C.J., Otten, T.G., Wilhelm, S.W., Wood, S.A., and Paerl, H.W. (2016) A review of the global ecology, genomics, and biogeography of the toxic cyanobacterium, *Microcystis* spp. *Harmful Algae* **54**: 4–20.
- Hasegawa, Y., Martin, J.L., Giewat, M.W., and Rooney-Varga, J.N. (2007) Microbial community diversity in the phycosphere of natural populations of the toxic alga, *Alexandrium fundyense*. *Environ Microbiol* **9**: 3108–3121.
- Hindák, F. (1996) Cyanophytes colonizing mucilage of chroococcal water blooms. *Beih Nova Hedwigia* **112**: 69–82.
- Hmelo, L., Van Mooy, B., and Mincer, T. (2012) Characterization of bacterial epibionts on the cyanobacterium *Trichodesmium*. *Aquat Microb Ecol* **67**: 1–14.
- Huisman, J., Codd, G.A., Paerl, H.W., Ibelings, B.W., Verspagen, J.M., and Visser, P.M. (2018) Cyanobacterial blooms. *Nat Rev Microbiol* **16**: 471–483.
- Jackrel, S.L., White, J.D., Evans, J.T., Buffin, K., Hayden, K., Sarnelle, O., and Deneff, V.J. (2019) Genome evolution and host microbiome shifts correspond with intraspecific niche divergence within harmful algal bloom-forming *Microcystis aeruginosa*. *Mol Ecol* **28**: 3994–4011.
- Jankowiak, J.G., and Gobler, C.J. (2020) The composition and function of microbiomes within *Microcystis* colonies are significantly different than native bacterial assemblages in two north American lakes. *Front Microbiol* **11**: 1016.
- Jasti, S., Sieracki, M.E., Poulton, N.J., Giewat, M.W., and Rooney-Varga, J.N. (2005) Phylogenetic diversity and specificity of bacteria closely associated with *Alexandrium* spp. and other phytoplankton. *Appl Environ Microbiol* **71**: 3483–3494. URL: <https://www.ncbi.nlm.nih.gov/pmc/articles/PMC1169014/pdf/2054-04.pdf>.
- Ježberová, J., and Komárková, J. (2007) Morphological transformation in a freshwater *Cyanobium* sp. induced by grazers. *Environ Microbiol* **9**: 1858–1862.
- Kardinaal, W.E.A., Janse, I., Kamst-van Agterveld, M., Meima, M., Snoek, J., Mur, L.R., et al. (2007) *Microcystis* genotype succession in relation to microcystin concentrations in freshwater lakes. *Aquat Microb Ecol* **48**: 1–12.
- Kim, M., Shin, B., Lee, J., Park, H.Y., and Park, W. (2019) Culture-independent and culture-dependent analyses of the bacterial community in the phycosphere of cyanobloom-forming *Microcystis aeruginosa*. *Sci Rep* **9**: 1–13.
- Kozich, J.J., Westcott, S.L., Baxter, N.T., Highlander, S. K., and Schloss, P.D. (2013) Development of a dual-index sequencing strategy and curation pipeline for analyzing amplicon sequence data on the MiSeq Illumina sequencing platform. *Appl Environ Microbiol* **79**: 5112–5120.
- Landa, M., Burns, A.S., Roth, S.J., and Moran, M.A. (2017) Bacterial transcriptome remodeling during sequential co-culture with a marine dinoflagellate and diatom. *ISME J* **11**: 2677–2690.
- Le Manach, S., Duval, C., Marie, A., Djediat, C., Catherine, A., Edery, M., et al. (2019) Global metabolomic characterizations of *Microcystis* spp. highlights clonal diversity in natural bloom-forming populations and expands metabolite structural diversity. *Front Microbiol* **10**: 791.
- Lee, M.D., Walworth, N.G., McParland, E.L., Fu, F.-X., Mincer, T.J., Levine, N.M., et al. (2017) The *Trichodesmium* consortium: conserved heterotrophic co-occurrence and genomic signatures of potential

- interactions. *ISME J* **11**: 1813–1824. <https://doi.org/10.1038/ismej.2017.49>.
- Li, M., Zhu, W., Gao, L., and Lu, L. (2013) Changes in extracellular polysaccharide content and morphology of *Microcystis aeruginosa* at different specific growth rates. *J Appl Phycol* **25**: 1023–1030.
- Lin, Y., Gifford, S., Ducklow, H., Schofield, O., and Cassar, N. (2019) Towards quantitative microbiome community profiling using internal standards. *Appl Environ Microbiol* **85**: e02634–e02618.
- Louati, I., Pascault, N., Debroas, D., Bernard, C., Humbert, J.-F., and Leloup, J. (2015) Structural diversity of bacterial communities associated with bloom-forming freshwater cyanobacteria differs according to the cyanobacterial genus. *PLoS One* **10**: e0140614.
- Ma, L., Calfee, B.C., Morris, J.J., Johnson, Z.I., and Zinser, E.R. (2018) Degradation of hydrogen peroxide at the ocean's surface: the influence of the microbial community on the realized thermal niche of *Prochlorococcus*. *ISME J* **12**: 473–484.
- Miller, T.R., Hnilicka, K., Dziedzic, A., Desplats, P., and Belas, R. (2004) Chemotaxis of *Silicibacter* sp. strain TM1040 toward dinoflagellate products. *Appl Environ Microbiol* **70**: 4692–4701.
- Mönnich, J., Tebben, J., Bergemann, J., Case, R., Wohlrab, S., and Harder, T. (2020) Niche-based assembly of bacterial consortia on the diatom *Thalassiosira rotula* is stable and reproducible. *ISME J*: **14**, 1614–1625. <https://doi.org/10.1038/s41396-020-0631-5>.
- Morris, J.J., Johnson, Z.I., Szul, M.J., Keller, M., and Zinser, E.R. (2011) Dependence of the cyanobacterium *Prochlorococcus* on hydrogen peroxide scavenging microbes for growth at the ocean's surface. *PLoS One* **6**: e16805.
- Oksanen, J., Blanchet, F. G., Kindt, R., Legendre, P., Minchin, P. R., O'hara, R. *et al.* (2013). *Package 'vegan'*. <https://cran.r-project.org/web/packages/vegan/vegan.pdf>.
- Otsuka, S., Suda, S., Li, R., Matsumoto, S., and Watanabe, M.M. (2000) Morphological variability of colonies of *Microcystis* morphospecies in culture. *J Gen Appl Microbiol* **46**: 39–50.
- Otten, T., Xu, H., Qin, B., Zhu, G., and Paerl, H. (2012) Spatiotemporal patterns and ecophysiology of toxigenic *Microcystis* blooms in Lake Taihu, China: implications for water quality management. *Environ Sci Technol* **46**: 3480–3488.
- Otten, T.G., Paerl, H.W., Dreher, T.W., Kimmerer, W.J., and Parker, A.E. (2017) The molecular ecology of *Microcystis* sp. blooms in the San Francisco estuary. *Environ Microbiol* **19**: 3619–3637.
- Ouellette, A.J., Handy, S.M., and Wilhelm, S.W. (2006) Toxic *Microcystis* is widespread in Lake Erie: PCR detection of toxin genes and molecular characterization of associated cyanobacterial communities. *Microb Ecol* **51**: 154–165.
- Paerl, H.W., and Gallucci, K.K. (1985) Role of chemotaxis in establishing a specific nitrogen-fixing cyanobacterial-bacterial association. *Science* **227**: 647–649.
- Parveen, B., Ravet, V., Djediat, C., Mary, I., Quiblier, C., Debroas, D., and Humbert, J.F. (2013) Bacterial communities associated with *Microcystis* colonies differ from free-living communities living in the same ecosystem. *Environ Microbiol Rep* **5**: 716–724.
- Pérez-Carrascal, O.M., Terrat, Y., Giani, A., Fortin, N., Greer, C.W., Tromas, N., and Shapiro, B.J. (2019) Coherence of *Microcystis* species revealed through population genomics. *ISME J* **13**: 2887–2900.
- Pruesse, E., Quast, C., Knittel, K., Fuchs, B.M., Ludwig, W., Peplies, J., and Glöckner, F.O. (2007) SILVA: a comprehensive online resource for quality checked and aligned ribosomal RNA sequence data compatible with ARB. *Nucleic Acids Res* **35**: 7188–7196.
- Raina, J.-B., Fernandez, V., Lambert, B., Stocker, R., and Seymour, J.R. (2019) The role of microbial motility and chemotaxis in symbiosis. *Nat Rev Microbiol* **17**: 284–294.
- Ribalet, F., Intertaglia, L., Lebaron, P., and Casotti, R. (2008) Differential effect of three polyunsaturated aldehydes on marine bacterial isolates. *Aquat Toxicol* **86**: 249–255.
- Rouco, M., Haley, S.T., and Dyhrman, S.T. (2016) Microbial diversity within the *Trichodesmium* holobiont. *Environ Microbiol* **18**: 5151–5160.
- Salter, S.J., Cox, M.J., Turek, E.M., Calus, S.T., Cookson, W.O., Moffatt, M.F., *et al.* (2014) Reagent and laboratory contamination can critically impact sequence-based microbiome analyses. *BMC Biol* **12**: 1–12.
- Sapp, M., Schwaderer, A.S., Wiltshire, K.H., Hoppe, H.-G., Gerds, G., and Wichels, A. (2007) Species-specific bacterial communities in the phycosphere of microalgae? *Microb Ecol* **53**: 683–699.
- Schloss, P. D., & Bishop, L. (2019). MiSeq Wet Lab SOP. URL https://github.com/SchlossLab/MiSeq_WetLab_SOP/blob/master/MiSeq_WetLab_SOP.md
- Schmidt, K.C., Jackrel, S.L., Smith, D.J., Dick, G.J., and Deneff, V.J. (2020) Genotype and host microbiome alter competitive interactions between *Microcystis aeruginosa* and *Chlorella sorokiniana*. *Harmful Algae* **99**, Article 101939. <https://doi.org/10.1016/j.hal.2020.101939>.
- Segev, E., Wyche, T.P., Kim, K.H., Petersen, J., Ellebrandt, C., Vlamakis, H., *et al.* (2016) Dynamic metabolic exchange governs a marine algal-bacterial interaction. *Elife* **5**: e17473.
- Seyedsayamdost, M.R., Case, R.J., Kolter, R., and Clardy, J. (2011) The Jekyll-and-Hyde chemistry of *Phaeobacter gallaeciensis*. *Nat Chem* **3**: 331–335. URL. <https://www.nature.com/articles/nchem.1002.pdf>.
- Seymour, J., Ahmed, T., Durham, W., and Stocker, R. (2010) Chemotactic response of marine bacteria to the extracellular products of *Synechococcus* and *Prochlorococcus*. *Aquat Microb Ecol* **59**: 161–168.
- Seymour, J.R., Amin, S.A., Raina, J.-B., and Stocker, R. (2017) Zooming in on the phycosphere: the ecological interface for phytoplankton-bacteria interactions. *Nat Microbiol* **2**: 1–12. <https://doi.org/10.1038/nmicrobiol.2017.65>.
- Sheik, C.S., Reese, B.K., Twing, K.I., Sylvan, J.B., Grim, S. L., Schrenk, M.O., *et al.* (2018) Identification and removal of contaminant sequences from ribosomal gene databases: lessons from the census of deep life. *Front Microbiol* **9**: 840.
- Shi, L., Huang, Y., Zhang, M., Shi, X., Cai, Y., Gao, S., *et al.* (2018) Large buoyant particles dominated by cyanobacterial colonies harbor distinct bacterial communities from small suspended particles and free-living bacteria in the water column. *Microbiol Open* **7**: e00608.

- Shia, L., Cai, Y., Wang, X., Li, P., Yu, Y., and Kong, F. (2010) Community structure of bacteria associated with *Microcystis* colonies from cyanobacterial blooms. *J Freshwater Ecol* **25**: 193–203.
- Sison-Mangus, M.P., Jiang, S., Tran, K.N., and Kudela, R.M. (2014) Host-specific adaptation governs the interaction of the marine diatom, *Pseudo-nitzschia* and their microbiota. *ISME J* **8**: 63–76.
- Smriga, S., Fernandez, V.I., Mitchell, J.G., and Stocker, R. (2016) Chemotaxis toward phytoplankton drives organic matter partitioning among marine bacteria. *Proc Natl Acad Sci* **113**: 1576–1581.
- Sonnenschein, E.C., Syit, D.A., Grossart, H.-P., and Ullrich, M.S. (2012) Chemotaxis of *Marinobacter adhaerens* and its impact on attachment to the diatom *Thalassiosira weissflogii*. *Appl Environ Microbiol* **78**: 6900–6907.
- Tu, J., Chen, L., Gao, S., Zhang, J., Bi, C., Tao, Y., et al. (2019) Obtaining genome sequences of mutualistic bacteria in single *Microcystis* colonies. *Int J Mol Sci* **20**: 5047.
- Van Mooy, B.A., Hmelo, L.R., Sofen, L.E., Campagna, S.R., May, A.L., Dyhrman, S.T., et al. (2012) Quorum sensing control of phosphorus acquisition in *Trichodesmium* consortia. *ISME J* **6**: 422–429.
- Wang, Q., Garrity, G.M., Tiedje, J.M., and Cole, J.R. (2007) Naive Bayesian classifier for rapid assignment of rRNA sequences into the new bacterial taxonomy. *Appl Environ Microbiol* **73**: 5261–5267.
- Westcott, S.L., and Schloss, P.D. (2017) OptiClust, an improved method for assigning amplicon-based sequence data to operational taxonomic units. *MSphere* **2**: e00073–e00017.
- Worm, J., and Søndergaard, M. (1998) Dynamics of heterotrophic bacteria attached to *Microcystis* spp. (cyanobacteria). *Aquat Microb Ecol* **14**: 19–28.
- Wynne, T.T., Stumpf, R.P., Tomlinson, M.C., Fahnenstiel, G. L., Dyble, J., Schwab, D.J., and Joshi, S.J. (2013) Evolution of a cyanobacterial bloom forecast system in western Lake Erie: development and initial evaluation. *J Great Lakes Res* **39**: 90–99.
- Xu, H., Cai, H., Yu, G., and Jiang, H. (2013) Insights into extracellular polymeric substances of cyanobacterium *Microcystis aeruginosa* using fractionation procedure and parallel factor analysis. *Water Res* **47**: 2005–2014.
- Zhang, K., Pan, R., Zhang, L., Zhang, T., and Fan, J. (2020) Interspecific competition between *Microcystis aeruginosa* and *Pseudanabaena* and their production of T&O compounds. *Chemosphere* **252**: 126509.
- Zhu, C.-M., Zhang, J.-Y., Guan, R., Hale, L., Chen, N., Li, M., et al. (2019) Alternate succession of aggregate-forming cyanobacterial genera correlated with their attached bacteria by co-pathways. *Sci Total Environ* **688**: 867–879.
- Zhu, W., Li, M., Luo, Y., Dai, X., Guo, L., Xiao, M., et al. (2014) Vertical distribution of *Microcystis* colony size in Lake Taihu: its role in algal blooms. *J Great Lakes Res* **40**: 949–955.

Supporting Information

Additional Supporting Information may be found in the online version of this article at the publisher's web-site:

Appendix S1. Supporting Information.

Appendix S2. Supporting Information.